



Published in final edited form as:

*Biochem J.* ; 474(23): 3903–3914. doi:10.1042/BCJ20170279.

## Rac1-stimulated macropinocytosis enhances G $\beta\gamma$ activation of PI3K $\beta$

Zahra Erami<sup>1,\*</sup>, Bassem D. Khalil<sup>1,\*</sup>, Gilbert Salloum<sup>1</sup>, Yanhua Yao<sup>1</sup>, Jaclyn LoPiccolo<sup>1</sup>, Aliaksei Shymanets<sup>2</sup>, Bernd Nürnberg<sup>2</sup>, Anne R. Bresnick<sup>3</sup>, and Jonathan M. Backer<sup>1,3</sup>

<sup>1</sup>Department of Molecular Pharmacology, Albert Einstein College of Medicine, Bronx, NY, U.S.A.

<sup>2</sup>Department of Pharmacology and Experimental Therapy, Institute for Pharmacology and Toxicology and Interfaculty Center of Pharmacogenomics and Pharma Research, Eberhard-Karls-Universität Tübingen, Tübingen, Germany

<sup>3</sup>Department of Biochemistry, Albert Einstein College of Medicine, Bronx, NY, U.S.A

### Abstract

Phosphoinositide 3-kinases (PI 3-kinases) are regulated by a diverse range of upstream activators, including receptor tyrosine kinases (RTKs), G-protein-coupled receptors (GPCRs), and small GTPases from the Ras, Rho and Rab families. For the Class IA PI 3-kinase PI3K $\beta$ , two mechanisms for GPCR-mediated regulation have been described: direct binding of G $\beta\gamma$  subunits to the C2-helical domain linker of p110 $\beta$ , and Dock180/Elmo1-mediated activation of Rac1, which binds to the Ras-Binding Domain of p110 $\beta$ . We now show that the integration of these dual pathways is unexpectedly complex. In breast cancer cells, expression of constitutively activated Rac1 (CA-Rac1) along with either GPCR stimulation or expression of G $\beta\gamma$  led to an additive PI3K $\beta$ -dependent activation of Akt. Whereas CA-Rac1-mediated activation of Akt was blocked in cells expressing a mutated PI3K $\beta$  that cannot bind G $\beta\gamma$ , G $\beta\gamma$  and GPCR-mediated activation of Akt was preserved when Rac1 binding to PI3K $\beta$  was blocked. Surprisingly, PI3K $\beta$ -dependent CA-Rac1 signaling to Akt was still seen in cells expressing a mutant p110 $\beta$  that cannot bind Rac1. Instead of directly binding to PI3K $\beta$ , CA-Rac1 acts by enhancing G $\beta\gamma$  coupling to PI3K $\beta$ , as CA-Rac1-mediated Akt activation was blocked by inhibitors of G $\beta\gamma$ . Cells expressing CA-Rac1 exhibited a robust induction of macropinocytosis, and inhibitors of macropinocytosis blocked the activation of Akt by CA-Rac1 or lysophosphatidic acid. Our data suggest that Rac1 can potentiate the activation of PI3K $\beta$  by GPCRs through an indirect mechanism, by driving the formation of macropinosomes that serve as signaling platforms for G $\beta\gamma$  coupling to PI3K $\beta$ .

Correspondence: Jonathan M. Backer (jonathan.backer@einstein.yu.edu) or Anne R. Bresnick (anne.bresnick@einstein.yu.edu).

\*These authors contributed equally to this work.

### Author Contribution

Z.E. and B.D.K. helped design the study and prepare the figures, contributed to the manuscript, and performed and analyzed experiments. G.S. performed and analyzed the macropinocytosis experiments. Y.Y. performed the experiments shown in Figure 2B. JLP purified the recombinant CA-Rac1. A.S. and B.N. purified the recombinant G $\beta\gamma$ . A.R.B. and J.M.B. conceived and co-ordinated the study and wrote the paper. All authors reviewed the results and approved the final version of the manuscript.

### Competing Interests

J.M.B. is on the Scientific Advisory board of Karus Therapeutics.

## Introduction

Class I PI 3-kinases comprise four distinct catalytic and seven distinct regulatory subunits. They mediate a wide range of non-redundant signaling events in distinct tissues and cell types [1]. PI3K $\beta$ , composed of either p85 $\alpha$  or p85 $\beta$  regulatory subunits and the p110 $\beta$  catalytic subunit, has been implicated in thrombosis, spermatogenesis, and tumorigenesis in tumors lacking the PTEN tumor suppressor [2–5]. At the cellular level, PI3K $\beta$  plays a role in vesicular trafficking, macroautophagy, and integrin signaling [3,4,6–8].

While all class I PI 3-kinases integrate activating and inhibitory inputs from multiple upstream regulators, the control of PI3K $\beta$  activity is particularly complex. PI3K $\beta$  is predicted to be strongly activated by receptor tyrosine kinases (RTKs) through SH2 domains in p85 [9]. PI3K $\beta$  is also activated by G-protein-coupled receptors (GPCRs), as G $\beta\gamma$  subunits from trimeric G-proteins bind directly to a surface loop in p110 $\beta$  [10]. G $\beta\gamma$  and tyrosine phosphorylated peptides show strong synergistic activation of PI3K $\beta$  *in vitro* [11]. However, several studies have shown that RTK activation of PI3K $\beta$  is weak relative to PI3K $\alpha$ , even in cells that contain similar levels of both isoforms [12,13]. The reason for this is not yet clear, but could reflect the specific targeting of PI3K $\beta$  to cellular regions that preclude its binding to RTKs. In contrast, studies in leukocytes show that PI3K $\beta$  is selectively responsive to a combined RTK-GPCR stimulus [14]. Finally, GPCRs can also activate PI3K $\beta$  through the Dock180/Elmo1-mediated activation of the small Rho GTPase Rac1, which binds to the Ras-Binding Domain (RBD) of p110 $\beta$  [15]. The ability of Rac1 (and Cdc42) to stimulate PI3K $\beta$  activity suggests that the activation of these GTPases downstream from RTKs might also activate PI3K $\beta$ , although this has not yet been tested.

Given the dual pathways by which GPCRs activate PI3K $\beta$ , we sought to examine the integration of these inputs in intact cells. Unlike previous studies in MEFs [15,16], we do not see a requirement for Rac1 binding to p110 $\beta$  during GPCR-mediated activation of PI3K $\beta$ . However, we have uncovered a novel mechanism for the effects of Rac1 on PI3K $\beta$ . Our data suggest that activated Rac1 drives the formation of macropinosomes, which enhance the coupling of G $\beta\gamma$  to PI3K $\beta$ . These studies highlight the increasingly complex biology of PI3K $\beta$  regulation in mammalian cells.

## Experimental procedures

### Antibodies and reagents

Mouse myc, rabbit pT308-Akt, and rabbit Akt antibodies were purchased from Cell Signaling Technology. Mouse FLAG, mouse GRK2, and mouse  $\alpha$ -tubulin antibodies were purchased from Sigma. Rabbit GFP antibody was a gift from Dr Erik Snapp, Janelia Research Campus, HHMI; in some figures GFP antibody was from Cell Signaling Technology. Lysophosphatidic acid (LPA) and epidermal growth factor (EGF) were purchased from Sigma–Aldrich and Millipore, respectively. Rhodamine phalloidin and 70 kDa Rhodamine Dextran were purchased from Invitrogen. 5-(*n*-Ethyl-*N*-isopropyl) amiloride (EIPA) and Latrunculin B were from Sigma–Aldrich and CalBiochem, respectively. The expression construct for GRKct-PM was a gift from Dr Philip Wedegaertner, Thomas Jefferson University. The mammalian expression constructs for GFP-

CA-Rac1 and GFP-DN-Rac1 were assembled by cloning eGFP and Rac1(Q61L) or Rac1(T17N), respectively, into pcDNA3.1 vectors.

### Cell lines and transfections

HEK293T cells and the human breast cancer cell line MDA-MB-231 were obtained from American Type Culture Collection (ATCC) and maintained in DMEM containing 10% FBS and supplemented with 100 U/ml penicillin and 100 µg/ml streptomycin. MDA-MB-231 knockdown cells, and cells in which endogenous p110β is replaced by physiological levels of murine wild-type p110β or a GPCR-uncoupled mutant (p110β<sup>KK-DD</sup>), have been previously described [17]. When indicated, stable p110β knockdown cells were transiently transfected with wild-type or mutant p110β, p110β<sup>KK-DD</sup>, or a Rac binding-deficient mutant (S205D/K224A; p110β<sup>RBD</sup>), using Lipofectamine 3000 (Thermo-Fisher) according to manufacturer instructions.

### Akt activation

Cells were transiently transfected with GFP-CA-Rac1 or a bicistronic vector encoding Gβγ using Lipofectamine 3000 as per manufacturer instructions. Alternatively, cells were starved for 18 h in serum-free medium supplemented with 0.1% BSA and then stimulated with 10 µM LPA for 5 min at 37°C. Cells were lysed in 2× Laemmli sample buffer with phosphatase inhibitor cocktails (Sigma–Aldrich and Calbiochem) and boiled for 5 min, and lysates were separated by SDS–PAGE and blotted as described. Blots were visualized using ECL (Thermo-Fisher) and quantitated by densitometry using ImageJ.

### Inhibitor treatments

When indicated, cells were transfected with GFP-DN-Rac1 or GRKct-PM 48 h prior to experiments. When indicated, cells were treated with TGX-221 (100 nM for 30 min prior to assay), pertussis toxin (200 ng/ml for 1 h prior to assay), EIPA (100 nM for 3 h prior to assay), or Latrunculin B (0.5 µM for 15 min prior to assay). Control cells in the TGX-221, EIPA, and Latrunculin B experiments were treated with 0.1% DMSO.

### EGF stimulation and phalloidin staining

MDA-MB-231 cells were plated on glass coverslips and transfected with the indicated plasmids. After 48 h, cells were starved for 18 h in serum-free medium supplemented with 0.1% BSA and stimulated with 5 nM EGF for 5 min at 37°C. Cells were then fixed with 4% paraformaldehyde, stained with rhodamine phalloidin, and imaged using a 1.4 N.A. 60× objective and a Nikon Eclipse fluorescence microscope.

### Protein purification

GST-CA-Rac1<sup>Q61L</sup> in pGEX6p-1 was transformed into BL21 *Escherichia coli* and protein expression was induced with 0.4 mM isopropyl β-D-thiogalactoside overnight at 18°C. Bacterial cells were harvested by centrifugation and pellets resuspended in 1× PBS containing 4 mM DTT, 2 mM EDTA, 2 mM PMSF, 2.5 units/ml nuclease (Thermo Scientific), and protease inhibitor tablets (Roche Diagnostics). The cells were sonicated and TritonX-100 was added to a final concentration of 1%. Lysates were rotated at 4°C for 20

min and centrifuged at  $27\,000 \times g$  for 15 min at  $4^{\circ}\text{C}$ . Cleared lysates were incubated with glutathione-agarose beads (Thermo Scientific) on a rotating wheel at  $4^{\circ}\text{C}$  for 2 h. The beads were washed three times in 50 mM Tris pH 8.0, 150 mM NaCl and stored in 50% glycerol at  $-20^{\circ}\text{C}$ . For use in kinase assays, CA-Rac1 was cleaved overnight at  $4^{\circ}\text{C}$  with PreScission Protease (GE Healthcare) in 50 mM Tris pH 8.0, 150 mM NaCl, 5 mM  $\text{MgCl}_2$ , and 1 mM DTT. The cleaved material was eluted, brought to 10% glycerol, and stored at  $-80^{\circ}\text{C}$ . Purification of heterologously expressed  $\text{G}\beta_1\gamma_2$  in Sf9 cells following infection with recombinant baculovirus has been recently described [18]. Proteins were stored at  $-80^{\circ}\text{C}$  until use.

### ***In vitro* binding assay**

HEK293T cells were transfected with murine or human myc-p110 $\beta^{\text{WT}}$  or myc-p110 $\beta^{\text{KK-DD}}$ . After 48 h, cells were lysed in 20 mM Tris pH 7.4, 150 mM NaCl, 5 mM  $\text{MgCl}_2$ , 1 mM DTT, 1% TritonX-100, and protease inhibitors. Glutathione beads containing GST or GST-CA-Rac1 were loaded with 2 mM GTP $\gamma\text{S}$  for 20 min at  $37^{\circ}\text{C}$  in loading buffer (20 mM Tris pH X.X, 5 mM EDTA, 25 mM EDTA, and 1 mM DTT).  $\text{MgCl}_2$  was then added at a final concentration of 10 mM, and the beads were placed on ice for 10 min. GST or GST-CA-Rac1 beads (~25  $\mu\text{g}$  of protein per sample) were added to cell lysates, and the samples were incubated on a rotating wheel at  $4^{\circ}\text{C}$  for 2 h. The beads were washed three times in lysis buffer, boiled in  $2\times$  Laemmli sample buffer, and analyzed on a 7.5% SDS-PAGE followed by blotting with a myc antibody.

### **Lipid kinase assay**

Myc-tagged human p110 $\beta$  and HA-tagged bovine p85 were co-expressed in HEK293T cells and immunopurified with myc antibodies and Protein G beads. The beads were washed with 40 mM HEPES pH 7.4, 0.1% BSA, 1 mM EGTA, 7 mM  $\text{MgCl}_2$ , 120 mM NaCl, 1 mM  $\beta$ -glycerophosphate, 1 mM DTT, and resuspended in 40  $\mu\text{l}$  of the same buffer. The beads were incubated in the presence of 45  $\mu\text{g}$  sonicated phosphatidylinositol and 100  $\mu\text{M}$  ATP containing 10  $\mu\text{Ci}$  [ $^{32}\text{P}$ ]-ATP, without or with 10  $\mu\text{M}$  Rac1, with shaking for 10 min. Reactions were stopped by the addition of 80  $\mu\text{l}$  of 3.2 M HCl and 160  $\mu\text{l}$  1 : 1 chloroform:methanol, vortexed, and centrifuged at  $13\,000\times g$  for 5 min. Lipids in the lower phase were separated by the thin layer chromatography in chloroform:methanol:water:ammonium hydroxide 60 : 47 : 11.3 : 2, and quantitated using a Molecular Dynamics Phosphorimager.

### **Macropinocytosis assay**

Acid washed 18 mm coverslips were rinsed twice with PBS and placed in 12-well plates. p110 $\beta$  knockdown cells transfected with wild-type p110 $\beta$ , p110 $\beta^{\text{KK-DD}}$ , or p110 $\beta^{\text{RBD}}$ , along with GFP-CA-Rac1 or GFP. After 48 h, cells were seeded at  $75 \times 10^3$  cells per coverslip in complete medium. Cells were pre-incubated with 0.1% DMSO or 25  $\mu\text{M}$  EIPA for 90 min, washed, and then incubated with 1 mg/ml 70 KDa rhodamine-Dextran for 30 min at  $37^{\circ}\text{C}$ . Cells were transferred to ice, washed five times with ice-cold PBS and fixed with 4% paraformaldehyde for 30 min at room temperature. Cells were then washed twice with  $1\times$  PBS, mounted on glass slides using DAPI Fluoromount-G $^{\text{®}}$  (SouthernBiotech),

sealed with nail polish and imaged immediately. Image acquisition was performed using a Nikon Eclipse fluorescence microscope equipped with phase contrast and rhodamine, DAPI and FITC filters. Images were acquired with a 40 $\times$ , 0.075 N.A. objective.

### Analysis of macropinosomes

Macropinosomes were analyzed by a modification of the method of Commisso et al. [19]. Briefly, images were analyzed in ImageJ. For a given experiment, a phase contrast image and corresponding fluorescence image with bright discrete macropinocytotic punctae were used to define analysis settings. The Set Scale function used the following parameters: distance in pixels: 620; known distance: 0.1; unit of length: mm. Background subtraction was performed using a rolling ball radius of 10 pixels. Images were adjusted using the Image:Adjust:Threshold commands, selecting Dark Background and Auto. The resulting thresholding was compared with a duplicate of the original image to make sure that all macropinosomes were selected, and manual adjustments were made to the threshold value, if necessary; the Apply function was then chosen. The outline of the cell was traced from the phase contrast image using the Polygon selections function, and this outline was superimposed on the thresholded fluorescent image. Finally, the number of macropinosomes was counted using the Analyze Particles function, using a Size setting of 0.00000044178-Infinity to select particles greater than 0.79  $\mu\text{m}$ . Thresholding settings from the first image were recorded and used for the analysis of subsequent images from the same data set.

### Statistical analysis

Statistical analyses were done using one-way ANOVA. A *P*-value less than 0.05 was considered statistically significant.

## Results

To study the integration of signaling from G $\beta\gamma$  and Rac1 by PI3K $\beta$ , we used stable MDA-MB-231 cells in which endogenous p110 $\beta$  is knocked down and replaced by physiological levels of wild-type p110 $\beta$  or a mutant (p110 $\beta^{\text{KK-DD}}$ ) that is defective for binding to G $\beta\gamma$  [17]. *In vitro*, this mutation has no effect on basal PI3K $\beta$  activity or activation by tyrosine phosphopeptides, but abolishes activation by G $\beta\gamma$  [10]. MDA-MB-231 cells expressing mutant PI3K $\beta$  show normal EGF-stimulated Akt activation but are defective for responses to GPCR ligands [17].

To produce comparable levels of Rac activation in cells expressing wild-type versus mutant p110 $\beta$ , we transfected the cells with constitutively active Rac1 (Rac1<sup>Q61L</sup>; CA-Rac1). Phosphorylation of Akt at T308 was used as readout for PI3K $\beta$  activation. In cells expressing wild-type PI3K $\beta$ , treatment with LPA or transfection of CA-Rac1 led to a two-fold increase in Akt phosphorylation, and Akt phosphorylation increased nearly four-fold when cells were stimulated with both CA-Rac1 and LPA (Figure 1A, B). LPA-stimulated Akt phosphorylation was markedly reduced in cells expressing GPCR-uncoupled PI3K $\beta$ , consistent with our previous work [17]. Surprisingly, stimulation of Akt phosphorylation by CA-Rac1 in cells expressing PI3K $\beta^{\text{KK-DD}}$  was also reduced, with no significant difference from untreated cells. The additive activation of Akt by LPA plus CA-Rac1 was reduced by

~60% in cells expressing GPCR-uncoupled p110 $\beta$ . Similar data were obtained when we transfected cells with recombinant G $\beta\gamma$  rather than stimulating with LPA. In cells expressing PI3K $\beta^{KK-DD}$ , activation of Akt by G $\beta\gamma$  and CA-Rac1, as well as the additive activation in cells expressing both G $\beta\gamma$  and CA-Rac1, were both inhibited (Figure 1C, D). To demonstrate that the activation of Akt by CA-Rac1 is a valid readout for activation of PI3K $\beta$ , we treated cells with the PI3K $\beta$ -specific inhibitor TGX-221. Akt activation by CA-Rac1 and additive activation by CA-Rac1 and LPA were both abolished by treatment with TGX-221 (Figure 1E, F).

Based on the structure of p110 $\beta$  [9], the binding sites for G $\beta\gamma$  (in the C2-helical linker) and Rac1 (in the RBD) reside in distinct domains of the protein, suggesting that a point mutation at one site should not affect binding at the other site. To confirm that mutation of the G $\beta\gamma$ -binding site did not affect Rac1 binding to the RBD, we measured the binding of recombinant PI3K $\beta$  to immobilized GST-CA-Rac1. Similar levels of wild-type and mutant PI3K $\beta$  bound to GST-CA-Rac1, but not GST beads (Figure 2A). We also measured the activation of recombinant PI3K $\beta$  by CA-Rac1 *in vitro* and observed a two-fold activation of both wild-type and mutant PI3K $\beta$  (Figure 2B). Therefore, the requirement for an intact G $\beta\gamma$  binding in p110 $\beta$  for Rac1 activation of PI3K $\beta$  is observed in cells but not *in vitro*.

The relationship between G $\beta\gamma$  and Rac during the activation of PI3K $\beta$  was not reciprocal, as LPA stimulation of Akt phosphorylation was unaffected by overexpression of dominant negative Rac1 (DN-Rac1) (Figure 3A). To confirm that the expression of DN-Rac1 was interfering with Rac1 signaling, we expressed GFP or GFP-DN-Rac1 in parental MDA-MB-231 cells and stimulated with EGF. Cells expressing GFP (Figure 3B; middle panel) and non-transfected cells (Figure 3B; right panel, open arrowheads) showed extensive membrane ruffling in response to EGF (compare to unstimulated cells in Figure 3B, left panel). In contrast, EGF-stimulated membrane ruffling was inhibited in cells expressing GFP-DN-Rac1 (Figure 3B; right panel, solid arrowheads).

We also measured LPA-stimulated Akt phosphorylation in MDA-MB-231 p110 $\beta$  knockdown cells transiently transfected with wild-type p110 $\beta$ , p110 $\beta^{KK-DD}$ , or a mutant p110 $\beta$  that is defective for binding to Rac1 (S205D/K224A [15]; p110 $\beta^{RBD}$ ). LPA stimulation of pT308-Akt was observed in cells expressing wild-type p110 $\beta$ , as well as in cells expressing the Rac1 binding-deficient p110 $\beta^{RBD}$  (Figure 3C, D). In contrast, the expression of GPCR-uncoupled p110 $\beta^{KK-DD}$  did not support Akt phosphorylation. These data show that in breast cancer cells, LPA stimulation of Akt does not require PI3K $\beta$  binding to Rac1.

We next tested whether loss of p110 $\beta$  binding to Rac1 would affect the activation of Akt by CA-Rac1. Surprisingly, despite the fact that CA-Rac1 activation of Akt was PI3K $\beta$  dependent (Figure 1F), we observed similar activation of Akt in p110 $\beta$  knockdown cells transiently expressing wild-type p110 $\beta$  versus p110 $\beta^{RBD}$  (Figure 4A, B). These data suggest that CA-Rac1 activates PI3K $\beta$  indirectly, by enhancing G $\beta\gamma$  coupling to PI3K $\beta$ . To test this model, we measured Akt phosphorylation in cells transfected with CA-Rac1 alone or with a membrane-targeted C-terminal fragment of the G $\beta\gamma$  effector GRK (GRKct-PM), which sequesters G $\beta\gamma$  subunits [20]. Activation of Akt by CA-Rac1 in serum-starved cells was



inhibited by ~50% in cells expressing GRKct-PM (Figure 4C, D). In an alternative approach, we measured CA-Rac1-mediated activation of Akt in serum-starved cells treated with pertussis toxin (PTX), which inhibits  $G\alpha_i$ -coupled GPCRs [21]. PTX caused a 40% decrease in Akt phosphorylation in cells expressing CA-Rac1 (Figure 4E, F). These two independent methods demonstrate that the activation of PI3K $\beta$  by CA-Rac1 requires  $G\beta\gamma$  signaling.

These data show that the expression of CA-Rac activates PI3K $\beta$  by a pathway that is independent of direct PI3K $\beta$ -Rac1 binding, but requires  $G\beta\gamma$ , and PI3K $\beta$  binding to  $G\beta\gamma$ . Interestingly, Swanson and colleagues have recently shown that macropinosomes can serve as signaling scaffolds for the propagation of GPCR signaling to PI3K [22]. Given that the expression of activated Rac1 stimulated the formation of macropinosomes in Raw 264.7 macrophages [23], we measured macropinocytosis in MDA-MB-231 cells transfected with CA-Rac1. Transfection of CA-Rac1 caused an increase in phase-bright cytosolic vesicles in cells expressing wild-type p110 $\beta$  (Figure 5A, upper panels), and CA-Rac1 caused a seven-fold increase in the uptake of 70 kDa rhodamine-dextran (Figure 5A, lower panels and Figure 5B); this uptake was blocked by the macropinocytosis inhibitor EIPA. CA-Rac1 stimulation of dextran uptake was somewhat reduced in cells expressing the Rac1-binding defective mutant of p110 $\beta$ , but still increased by three-fold (Figure 5B). Notably, activation of Akt by the expression of CA-Rac1 was blocked by the treatment of cells with EIPA (Figure 6A, B) or another the macropinocytosis inhibitor, Latrunculin B (Figure 6C, D). Similarly, LPA stimulation of Akt was blocked by EIPA (Figure 6E, F). Thus, both GPCR- and CA-Rac1-mediated activation of Akt requires macropinocytosis, which acts by enhancing  $G\beta\gamma$  coupling to PI3K $\beta$ .

## Discussion

The regulation of the PI3K $\beta$  isoform of Class IA PI 3-kinase is unusually complex, given its ability to directly bind small GTPases (Rac1, Cdc42, Rab5, though the RBD and helical domains [15,24],  $G\beta\gamma$  (through the C2-helical linker [10]) and tyrosine phosphorylated proteins (through its p85 regulatory subunit). Previous studies in MEFs have focused on the coupling between Rac- and  $G\beta\gamma$ -mediated activation at the level of p110 $\beta$  itself, and have suggested the existence of a feed-forward loop involving Rac1-mediated activation of PI3K $\beta$ - and PI3K $\beta$ -mediated activation of Rac1 [25], as well as the enhancement of GPCR signaling to PI3K $\beta$  by Rac1-mediated targeting of PI3K $\beta$  to lipid rafts [16]. The present study identifies another layer of regulation, in which Rac1-stimulated macropinosomes enhance  $G\beta\gamma$  coupling to PI3K $\beta$  independently of Rac1 binding to p110 $\beta$ .

We have previously shown that GPCR signaling in PI3K $\beta$  in MDA-MB-231 cells is required for tumor cell invasion and metastasis, but not for tumor cell growth [17]. To better understand the roles of Rac1 and  $G\beta\gamma$  in the regulation of PI3K $\beta$  in breast cancer cells, we used T308 phosphorylation of Akt as a readout for PI3K $\beta$  activity in p110 $\beta$  knockdown cells expressing physiological levels of wild-type or mutant p110 $\beta$ . We examined activation by both a GPCR ligand (LPA) and expression of constitutively active Rac1 (CA-Rac1). This latter approach was used to avoid potential effects of p110 $\beta$  mutants on the activation of endogenous Rac1. Importantly, experiments with TGX-221 showed that in MDA-MB-231

cells, activation of Akt by LPA or CA-Rac1 is dependent on PI3K $\beta$ , validating our use of pT308-Akt as a reporter. While an appropriate assay in breast cancer cells, this approach may not be useful in cells of hematopoietic origin (e.g. macrophages and neutrophils), which also express high levels of PI3K $\gamma$ . Indeed, GPCR stimulation of PIP<sub>3</sub> in macrophages is largely PI3K $\gamma$  dependent [14]. Although MDA-MB-231 cells do express PI3K $\gamma$  [26], this isoform does not appear to contribute significantly to GPCR signaling to Akt in these cells.

Stimulation of MDA-MB-231 cells with CA-Rac1 and LPA, or overexpression of G $\beta\gamma$ , led to additive stimulation of Akt. However, the effect of mutations in the G $\beta\gamma$ - and Rac1-binding sites in p110 $\beta$  was not reciprocal. Mutation of the G $\beta\gamma$ -binding site caused a loss of G $\beta\gamma$ - and LPA-stimulated Akt activation, as well as a loss of Rac1-mediated activation. In contrast, mutation of the Rac1-binding site in p110 $\beta$ , or expression of dominant negative Rac1, had no effect on G $\beta\gamma$ -mediated Akt activation. Even more surprising, mutation of the Rac1-binding domain in p110 $\beta$  had no effect on the activation of Akt by either LPA or CA-Rac.

Studies in MEFs have revealed dual pathways for PI3K $\beta$  activation by GPCRs, involving either direct binding of G $\beta\gamma$  to PI3K $\beta$  [10] or G $\beta\gamma$ -stimulation of the ELMO/DOCK/Rac1 pathway, which leads to the binding of activated Rac1 to PI3K $\beta$  [15] and targeting of PI3K $\beta$  to lipid rafts [16]. For unclear reasons, we cannot detect a requirement for Rac1 binding during LPA-stimulated activation of PI3K $\beta$  in MDA-MB-231 cells. This could be due either to differences in the expression/activity of ELMO/DOCK, or other differences between MEFs and breast cancer cells. Lipid raft-mediated signaling has been documented in MDA-MB-231 cells [27], but our data suggest that Rac1-mediated targeting of PI3K $\beta$  to lipid rafts is not critical for G $\beta\gamma$ - or GPCR-mediated PI3K $\beta$  activation in MDA-MB-231 cells.

The finding that the activation of PI3K $\beta$  by CA-Rac1 does not require an intact Rac1-binding site in p110 $\beta$  clearly indicates an indirect mechanism for Rac1 activation of PI3K $\beta$ . However, this mechanism is specific for GPCR signaling to PI3K $\beta$ , as Rac1-mediated activation is blocked by the mutation of the G $\beta\gamma$ -binding site in p110 $\beta$ , treatment of cells with PTX, or expression of GRKct-PM, which sequesters endogenous G $\beta\gamma$  subunits.

How might Rac1 activation enhance G $\beta\gamma$  coupling to PI3K $\beta$ ? Rac could work by inhibiting a GRK or other G $\alpha_i$  GAP so as to prolong GPCR-stimulated G $\beta\gamma$  signaling, although this would be unlikely to affect signaling by overexpressed G $\beta\gamma$ . Alternatively, studies by Swanson and colleagues have proposed that macropinocytotic cups can serve as signaling platforms that enhance GPCR signaling. In bone marrow-derived macrophages, inhibitors of macropinocytosis block stimulation of Akt by the CXCR4 receptor, and both PIP<sub>3</sub> and phosphorylated Akt can be detected in macropinocytotic cups that form in CXCL12-stimulated bone marrow-derived macrophages [22]. In MDA-MB-231 cells expressing wild-type p110 $\beta$ , the expression of CA-Rac1 causes a large increase in the production of phase-bright vesicles, and a seven-fold stimulation of macropinocytosis. Moreover, the activation of Akt by CA-Rac1 is blocked by treatment with the macropinocytosis inhibitor EIPA, or disruption of the actin cytoskeleton with Latrunculin B, which also blocks macropinocytosis. EIPA also blocks the activation of Akt by LPA, demonstrating a requirement for macropinocytosis during physiological regulation of GPCR signaling to PI3K $\beta$ . Of note,



while the effects of amiloride (the parent compound of EIPA) on EGF-stimulated macropinocytosis in A431 cells involve the inhibition of Rac activation [28], this would not be affect signaling in cells expressing constitutively active Rac1.

In the present study, we focused on GPCR signaling to PI3K $\beta$ . It has been suggested that signaling by RTKs like the CSF-1R can also be enhanced by macropinosomes formation, but only at low levels of ligand stimulation [22]. However, PI3K $\beta$  does not appear to couple effectively to RTKs [12–14], so we have not pursued the role of macropinosomes in RTK/PI3K $\beta$  signaling. In contrast, studies in neutrophils and macrophages have shown that PI3K $\beta$  can serve as a coincidence detector from simultaneous RTK-GPCR stimuli [14]. A potential role for macropinosomes in responses to a combined RTK-GPCR stimulus in breast cancer cells remains an interesting question.

The role of macropinosomes (or macropinocytotic cups) in enhancing G $\beta\gamma$  signaling to PI3K $\beta$  that we observe in breast cancer cells has some parallels to the requirement for lipid raft targeting of PI3K $\beta$  described in MEFs [16]. In both cases, a membrane subdomain enhances the interaction between PI3K $\beta$  and G $\beta\gamma$ . The need for a membrane based amplification system may be inherent in the p110 $\beta$ -G $\beta\gamma$  interaction, which is relatively weak compared with that of PI3K $\gamma$  and G $\beta\gamma$ , and only occurs on membranes [10]. A major difference in the two systems is that in MEFs, targeting of PI3K $\beta$  to rafts requires a direct Rac1-PI3K $\beta$  interaction, whereas in breast cancer cells, Rac1 is required to produce the macropinocytotic cup, but its direct binding to PI3K $\beta$  is not required. The precise mechanisms that target G $\beta\gamma$ , PI3K $\beta$  or both to macropinocytotic cups will be an important avenue for future investigation.

## Acknowledgments

### Funding

This manuscript was supported by NIH grants GM112524 and CA100324, and by the Albert Einstein College of Medicine Cancer Center [P30 CA013330], and by the Deutsche Forschungsgemeinschaft (DFG).

We thank Dr Philip Wedegaertner, Thomas Jefferson University, for the GRKct-PM construct, and Drs Joel Swanon, University of Michigan, and Sergio Grinstein, Hospital for Sick Kids, Toronto, for helpful discussions and suggestions.

## Abbreviations

<b>ATCC</b>	American Type Culture Collection
<b>EGF</b>	epidermal growth factor
<b>EIPA</b>	5-( <i>n</i> -ethyl- <i>N</i> -isopropyl) amiloride
<b>GPCRs</b>	G-protein-coupled receptors
<b>LPA</b>	lysophosphatidic acid
<b>MEFs</b>	mouse embryonic fibroblasts
<b>RBD</b>	Ras-Binding Domain

**RTKs** receptor tyrosine kinases

## References

1. Backer JM. The regulation of class IA PI 3-kinases by inter-subunit interactions. *Curr Top Microbiol Immunol.* 2010; 346:87–114. [PubMed: 20544340]
2. Cirao E, Morello F, Hobbs RM, Wolf F, Marone R, Iezzi M, et al. Essential role of the p110 $\beta$  subunit of phosphoinositide 3-OH kinase in male fertility. *Mol Biol Cell.* 2010; 21:704–711. <https://doi.org/10.1091/mbc.E09-08-0744>. [PubMed: 20053680]
3. Jackson SP, Schoenwaelder SM, Goncalves I, Nesbitt WS, Yap CL, Wright CE, et al. PI 3-kinase p110 $\beta$ : a new target for antithrombotic therapy. *Nat Med.* 2005; 11:507–514. <https://doi.org/10.1038/nm1232>. [PubMed: 15834429]
4. Jia S, Liu Z, Zhang S, Liu P, Zhang L, Lee SH, et al. Essential roles of PI(3)K-p110 $\beta$  in cell growth, metabolism and tumorigenesis. *Nature.* 2008; 454:776–779. [PubMed: 18594509]
5. Wee S, Wiederschain D, Maira SM, Loo A, Miller C, deBeaumont R, et al. PTEN-deficient cancers depend on PIK3CB. *Proc Natl Acad Sci U S A.* 2008; 105:13057–13062. <https://doi.org/10.1073/pnas.0802655105>. [PubMed: 18755892]
6. Cirao E, Iezzi M, Marone R, Marengo S, Curcio C, Costa C, et al. Phosphoinositide 3-kinase p110 $\beta$  activity: key role in metabolism and mammary gland cancer but not development. *Sci Signal.* 2008; 1:ra3. <https://doi.org/10.1126/scisignal.1161577>. [PubMed: 18780892]
7. Gratacap MP, Guillermet-Guibert J, Martin V, Chicanne G, Tronchère H, Gaits-Iacovoni F, et al. Regulation and roles of PI3K $\beta$ , a major actor in platelet signaling and functions. *Adv Enzyme Regul.* 2011; 51:106–116. <https://doi.org/10.1016/j.advenzreg.2010.09.011>. [PubMed: 21035500]
8. Dou Z, Pan JA, Dbouk HA, Ballou LM, DeLeon JL, Fan Y, et al. Class IA PI3K p110 $\beta$  subunit promotes autophagy through Rab5 small GTPase in response to growth factor limitation. *Mol Cell.* 2013; 50:29–42. <https://doi.org/10.1016/j.molcel.2013.01.022>. [PubMed: 23434372]
9. Zhang X, Vadas O, Perisic O, Anderson KE, Clark J, Hawkins PT, et al. Structure of lipid kinase p110 $\beta$ /p85 $\beta$  elucidates an unusual SH2-domain-mediated inhibitory mechanism. *Mol Cell.* 2011; 41:567–578. <https://doi.org/10.1016/j.molcel.2011.01.026>. [PubMed: 21362552]
10. Dbouk HA, Vadas O, Shymanets A, Burke JE, Salamon RS, Khalil BD, et al. G protein-coupled receptor-mediated activation of p110 $\beta$  by G $\beta\gamma$  is required for cellular transformation and invasiveness. *Sci Signal.* 2012; 5:ra89. <https://doi.org/10.1126/scisignal.2003264>. [PubMed: 23211529]
11. Maier U, Babich A, Nürnberg B. Roles of non-catalytic subunits in G $\beta\gamma$ -induced activation of class I phosphoinositide 3-kinase isoforms  $\beta$  and  $\gamma$ . *J Biol Chem.* 1999; 274:29311–29317. <https://doi.org/10.1074/jbc.274.41.29311>. [PubMed: 10506190]
12. Knight ZA, Gonzalez B, Feldman ME, Zunder ER, Goldenberg DD, Williams O, et al. A pharmacological map of the PI3-K family defines a role for p110 $\alpha$  in insulin signaling. *Cell.* 2006; 125:733–747. <https://doi.org/10.1016/j.cell.2006.03.035>. [PubMed: 16647110]
13. Guillermet-Guibert J, Bjorklof K, Salpekar A, Gonella C, Ramadani F, Bilancio A, et al. The p110 $\beta$  isoform of phosphoinositide 3-kinase signals downstream of G protein-coupled receptors and is functionally redundant with p110 $\gamma$ . *Proc Natl Acad Sci U S A.* 2008; 105:8292–8297. <https://doi.org/10.1073/pnas.0707761105>. [PubMed: 18544649]
14. Houslay DM, Anderson KE, Chessa T, Kulkarni S, Fritsch R, Downward J, et al. Coincident signals from GPCRs and receptor tyrosine kinases are uniquely transduced by PI3K $\beta$  in myeloid cells. *Sci Signal.* 2016; 9:ra82. <https://doi.org/10.1126/scisignal.aae0453>. [PubMed: 27531651]
15. Fritsch R, de Krijger I, Fritsch K, George R, Reason B, Kumar MS, et al. RAS and RHO families of GTPases directly regulate distinct phosphoinositide 3-kinase isoforms. *Cell.* 2013; 153:1050–1063. <https://doi.org/10.1016/j.cell.2013.04.031>. [PubMed: 23706742]
16. Cizmecioglu O, Ni J, Xie S, Zhao JJ, Roberts TM. Rac1-mediated membrane raft localization of PI3K/p110 $\beta$  is required for its activation by GPCRs or PTEN loss. *eLife.* 2016; 5:776. <https://doi.org/10.7554/eLife.17635>.

17. Khalil BD, Hsueh C, Cao Y, Abi Saab WF, Wang Y, Condeelis JS, et al. GPCR signaling mediates tumor metastasis via PI3K $\beta$ . *Cancer Res.* 2016; 76:2944–2953. <https://doi.org/10.1158/0008-5472.CAN-15-1675>. [PubMed: 27013201]
18. Shymanets A, Prajwal, Vadas O, Czupalla C, LoPiccolo J, Brenowitz M, et al. Different inhibition of G $\beta\gamma$ -stimulated class IB phosphoinositide 3-kinase (PI3K) variants by a monoclonal antibody. Specific function of p101 as a G $\beta\gamma$ -dependent regulator of PI3K $\gamma$  enzymatic activity. *Biochem J.* 2015; 469:59–69. <https://doi.org/10.1042/BJ20150099>. [PubMed: 26173259]
19. Commisso C, Flinn RJ, Bar-Sagi D. Determining the macropinocytic index of cells through a quantitative image-based assay. *Nat Protoc.* 2014; 9:182–192. <https://doi.org/10.1038/nprot.2014.004>. [PubMed: 24385148]
20. Irannejad R, Wedegaertner PB. Regulation of constitutive cargo transport from the *trans*-Golgi network to plasma membrane by Golgi-localized G protein  $\beta\gamma$  subunits. *J Biol Chem.* 2010; 285:32393–32404. <https://doi.org/10.1074/jbc.M110.154963>. [PubMed: 20720014]
21. Smrcka AV. G protein  $\beta\gamma$  subunits: central mediators of G protein-coupled receptor signaling. *Cell Mol Life Sci.* 2008; 65:2191–2214. <https://doi.org/10.1007/s00018-008-8006-5>. [PubMed: 18488142]
22. Pacitto R, Gaeta I, Swanson JA, Yoshida S. CXCL12-induced macropinocytosis modulates two distinct pathways to activate mTORC1 in macrophages. *J Leukoc Biol.* 2017; 101:683–692. <https://doi.org/10.1189/jlb.2A0316-141RR>. [PubMed: 28250113]
23. Fujii M, Kawai K, Egami Y, Araki N. Dissecting the roles of Rac1 activation and deactivation in macropinocytosis using microscopic photo-manipulation. *Sci Rep.* 2013; 3:2385. <https://doi.org/10.1038/srep02385>. [PubMed: 23924974]
24. Salamon RS, Dbouk HA, Collado D, Lopiccolo J, Bresnick AR, Backer JM. Identification of the Rab5 binding site in p110 $\beta$ : assays for PI3K $\beta$  binding to Rab5. *Methods Mol Biol.* 2015; 1298:271–281. [https://doi.org/10.1007/978-1-4939-2569-8\\_23](https://doi.org/10.1007/978-1-4939-2569-8_23). [PubMed: 25800850]
25. Yuzugullu H, Baitsch L, Von T, Steiner A, Tong H, Ni J, et al. A PI3K p110 $\beta$ –Rac signalling loop mediates Pten-loss-induced perturbation of haematopoiesis and leukaemogenesis. *Nat Commun.* 2015; 6:8501. <https://doi.org/10.1038/ncomms9501>. [PubMed: 26442967]
26. Brazzatti JA, Klingler-Hoffmann M, Haylock-Jacobs S, Harata-Lee Y, Niu M, Higgins MD, et al. Differential roles for the p101 and p84 regulatory subunits of PI3K $\gamma$  in tumor growth and metastasis. *Oncogene.* 2012; 31:2350–2361. <https://doi.org/10.1038/onc.2011.414>. [PubMed: 21996737]
27. Badana A, Chintala M, Varikuti G, Pudi N, Kumari S, Kappala VR, et al. Lipid raft integrity is required for survival of triple negative breast cancer cells. *J Breast Cancer.* 2016; 19:372–384. <https://doi.org/10.4048/jbc.2016.19.4.372>. [PubMed: 28053625]
28. Koivusalo M, Welch C, Hayashi H, Scott CC, Kim M, Alexander T, et al. Amiloride inhibits macropinocytosis by lowering submembranous pH and preventing Rac1 and Cdc42 signaling. *J Cell Biol.* 2010; 188:547–563. <https://doi.org/10.1083/jcb.200908086>. [PubMed: 20156964]

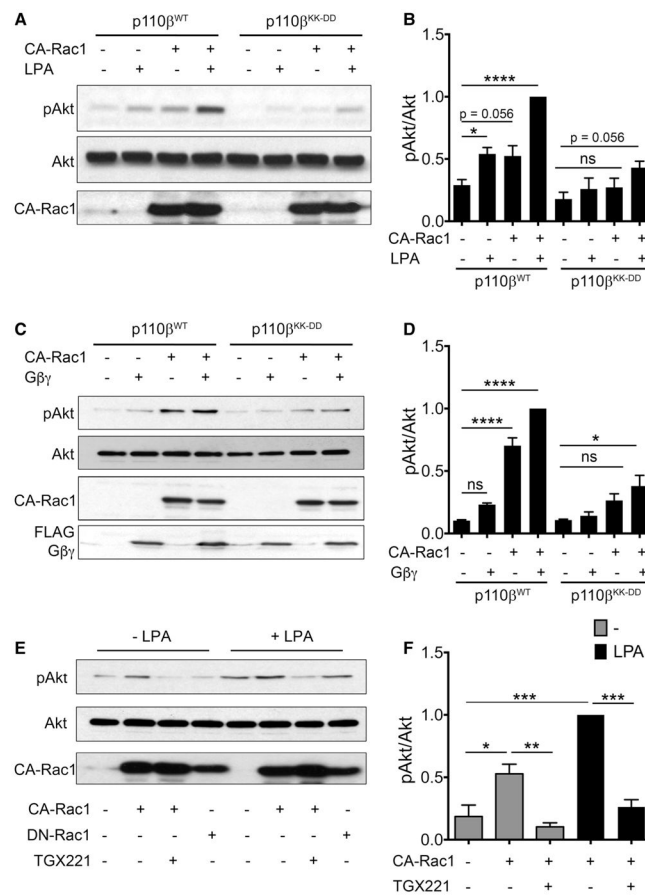


**Figure 1. CA-Rac1 does not activate GPCR-uncoupled p110β**

(A) MDA-MB-231 cells stably expressing wild-type or GPCR uncoupled p110β (p110β<sup>KK-DD</sup>) were transiently transfected with control plasmid or GFP-CA-Rac1, and stimulated with or without 10 μM LPA for 5 min. Representative immunoblots show pT308-Akt, total Akt, and GFP-CA-Rac1. (B) Quantitation of pAkt/Akt ratios from immunoblots in (A). pAkt/Akt ratios in each experiment were normalized to that seen in LPA-stimulated cells expressing wild-type p110β and GFP-CA-Rac1. The data represent the mean ± SEM from four independent experiments. (C) MDA-MB-231 cells stably expressing wild-type p110β or p110β<sup>KK-DD</sup> were transiently transfected with control plasmid, GFP-CA-Rac1, and/or Flag-Gβγ plasmids. Representative immunoblots show pT308-Akt, total Akt, GFP-CA-Rac1, and Flag-Gβγ. (D) Quantitation of pAkt/Akt ratios from immunoblots in (C). pAkt/Akt ratios in each experiment were normalized to that seen in cells simultaneously expressing wild-type p110β, GFP-CA-Rac1, and Gβγ. The data represent the mean ± SD from two independent experiments. (E) Parental MDA-MB-231 cells were transiently transfected with GFP-CA-Rac1 or GFP-DN-Rac1, and stimulated with LPA and treated with TGX-221 as indicated. Representative immunoblots show pT308-Akt, total Akt, and GFP-CA-Rac1. (F) Quantitation of pAkt/Akt ratios from (E) pAkt/Akt ratios in each experiment were normalized to that seen in cells expressing GFP-CA-Rac1 without TGX-221 treatment. Quantitation of the DN-Rac1 data in (E) is shown in Figure 3A. \*P < 0.05; \*\*P < 0.01; \*\*\*P < 0.0001; ns: not significant.

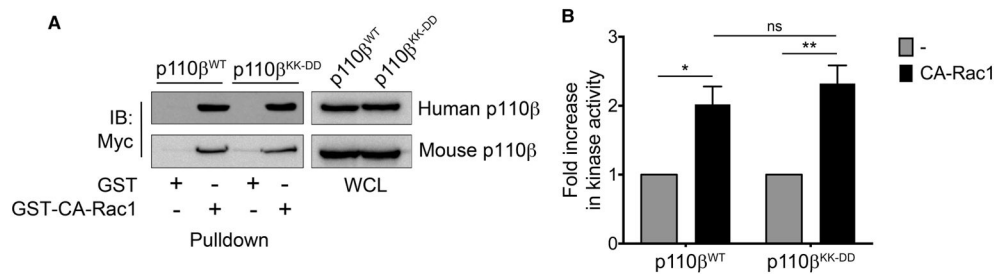


**Figure 2. GPCR-uncoupled p110β binds and is activated by CA-Rac1 *in vitro***  
**(A)** Representative immunoblots showing binding of human (upper panel) and mouse (lower panel) myc-tagged wild-type p110β or p110β<sup>KK-DD</sup> to GST or GST-CA-Rac1 beads. **(B)** *In vitro* lipid kinase activity of human wild-type p110β or p110β<sup>KK-DD</sup> with or without 10 μM recombinant GST-CA-Rac1. Values were normalized to those obtained for each protein in the absence of GFP-CA-Rac1. The data represent the mean ± SEM from three independent experiments. \**P* < 0.05; \*\**P* < 0.01; ns: not significant.

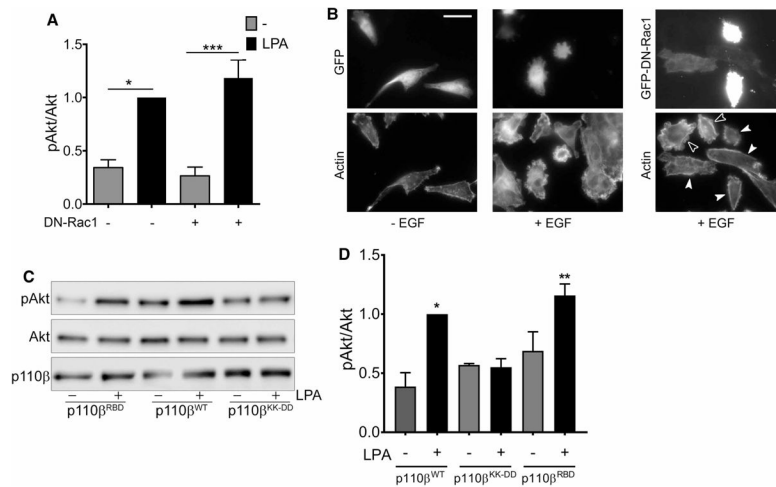


**Figure 3. LPA-stimulated activation of PI3K $\beta$  does not require Rac1 binding**

(A) Parental MDA-MB-231 cells were transfected with GFP or GFP-DN-Rac1 and stimulated with or without 10  $\mu$ M LPA for 5 min. pAkt/Akt ratios in each experiment were normalized to that seen in LPA-stimulated cells without DN-Rac1. The data represent the mean  $\pm$  SEM from three independent experiments. Western blot data from one of the three experiments is shown in Figure 1E. (B) Representative micrographs of parental MDA-MB-231 cells transfected with GFP or GFP-DN-Rac1 (upper panels) and stimulated without or with EGF. Cells were stained with rhodamine phalloidin to visualize F-actin (lower panels). Open arrowheads indicate untransfected cells that show membrane ruffling. Closed arrowheads show transfected cells with reduced ruffling. Scale bar = 50  $\mu$ m. (C) Stable p110 $\beta$  knockdown cells were transiently transfected with wild-type p110 $\beta$ , p110 $\beta$ <sup>KK-DD</sup>, or p110 $\beta$ <sup>RBD</sup>. Forty-eight hours after transfection, cells were starved overnight and then stimulated with 10  $\mu$ M LPA for 5 min. Cells were lysed and blotted for p110 $\beta$ , Akt, and pT308-Akt. (D) Quantitation of pAkt/Akt immunoblots in Figure 3D. pAkt/Akt ratios in each experiment were normalized to that seen in cells expressing wild-type p110 $\beta$  and stimulated with LPA. The data represent the mean  $\pm$  SEM from three independent experiments. \* $P$  < 0.05; \*\* $P$  < 0.01; \*\*\* $P$  < 0.001; ns: not significant.



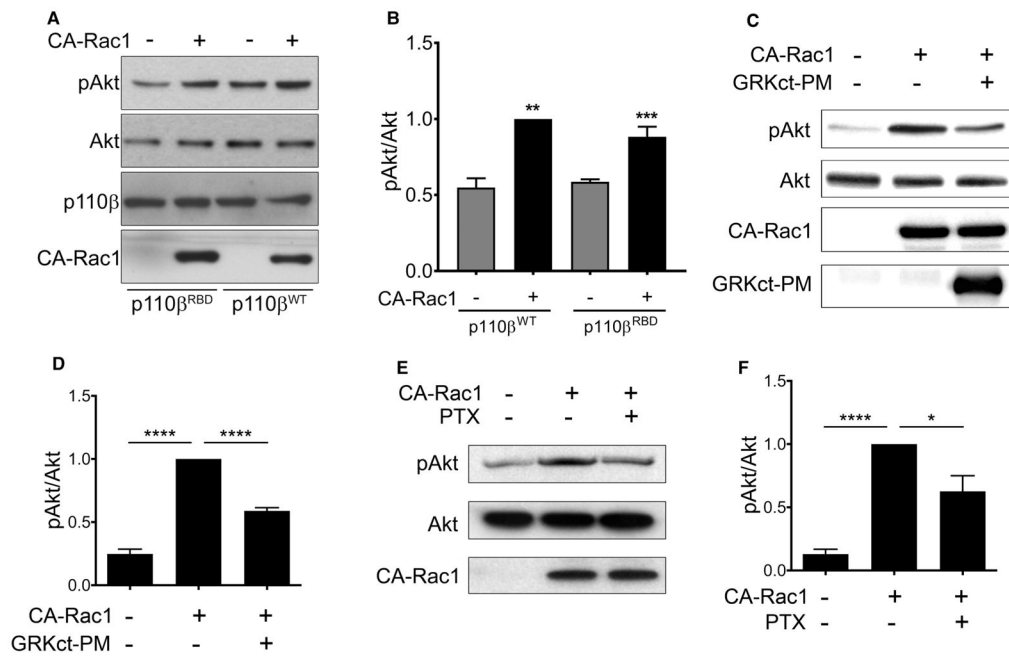


**Figure 4. CA-Rac1-mediated activation of PI3Kβ requires Gβγ**

(A) Stable p110β knockdown cells were transiently transfected with wild-type p110β, p110β<sup>KK-DD</sup> or p110β<sup>RBD</sup>, with or without GFP-CA-Rac1. After 48 h, cells were lysed and blotted for p110β, Akt, and pT308-Akt. (B) Quantitation of pAkt/Akt immunoblots in (A). pAkt/Akt ratios in each experiment were normalized to that seen in cells expressing wild-type p110β and GFP-CA-Rac1. The data represent the mean ± SEM from three independent experiments. (C) Parental MDA-MB-231 cells were transfected with GFP-CA-Rac1 with or without co-transfection of GRKct-PM. Representative immunoblots show pT308-Akt, total Akt, GFP-CA-Rac1, and GRKct-PM. (D) Quantitation of pAkt/Akt levels from immunoblots in (C). pAkt/Akt ratios in each experiment were normalized to that seen in cells expressing GFP-CA-Rac1 without GRKct-PM. The data represent the mean ± SEM from five independent experiments. (E) MDA-MB-231 cells were transfected with GFP-CA-Rac1 with or without PTX treatment. Representative immunoblots show pT308-Akt, total Akt, and GFP-CA-Rac1. (F) Quantitation of pAkt/Akt levels from immunoblots in (E). pAkt/Akt ratios in each experiment were normalized to that seen in cells transfected with GFP-CA-Rac1 without PTX treatment. The data represent the mean ± SEM from three independent experiments. \**P* < 0.05; \*\*\*\**P* < 0.0001.

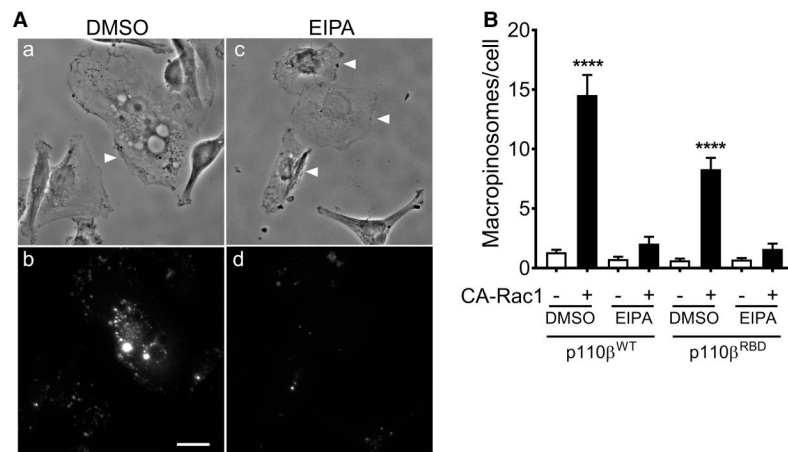


**Figure 5. CA-Rac1 stimulates macropinocytosis**

(A) Stable p110 $\beta$  knockdown cells were transfected with wild-type p110 $\beta$  and GFP-CA-Rac1. After 48 h, cells were pretreated with 0.1% DMSO or 25  $\mu$ M EIPA for 90 min, incubated with 1 mg/ml 70 kDa rhodamine-Dextran for 30 min at 37°C, fixed and imaged. (B) Stable p110 $\beta$  knockdown cells were transfected with wild-type p110 $\beta$  or p110 $\beta$ <sup>RBD</sup>, with or without GFP-CA-Rac1. The number of macropinosomes per cell (defined as vesicles greater than 0.75  $\mu$ m in diameter) in GFP-positive cells were counted as described in the Experimental Procedures. Scale bar = 20  $\mu$ m.

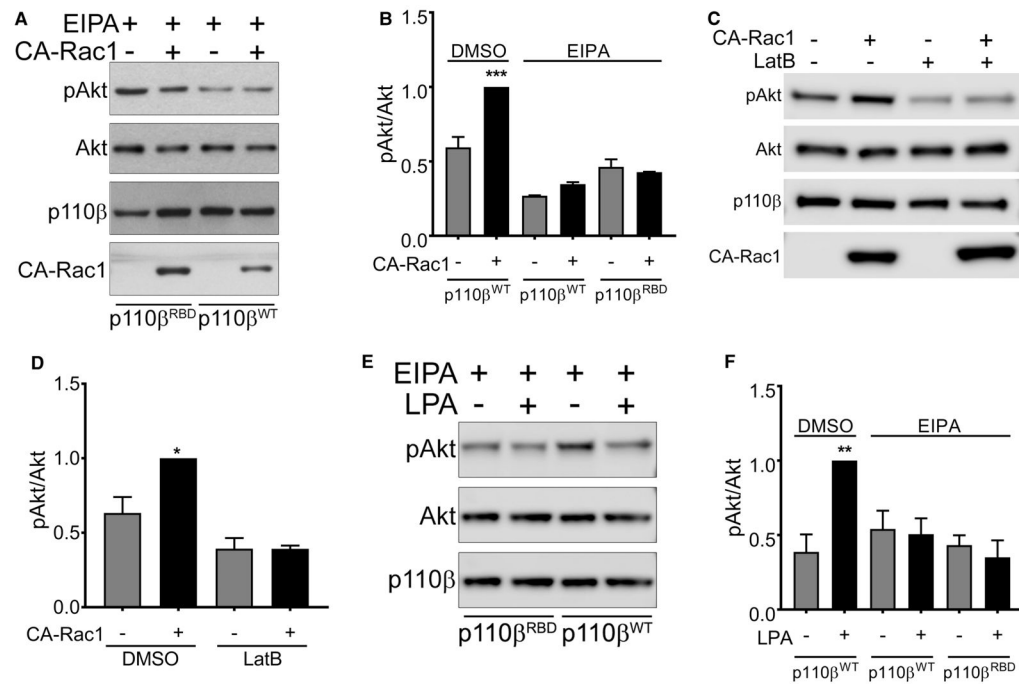


### Figure 6. Stimulation of PI3K $\beta$ by CA-Rac1 and LPA requires macropinocytosis

(A) Stable p110 $\beta$  knockdown cells were transiently transfected with wild-type p110 $\beta$ , p110 $\beta^{KK-DD}$  or p110 $\beta^{RBD}$ , without or with GFP-CA-Rac1. After 48 h, cells were treated with 25  $\mu$ M EIPA for 3 h, lysed and blotted for p110 $\beta$ , Akt and pT308-Akt. (B) Quantitation of pAkt/Akt immunoblots in Figure 6A. The data represent the mean  $\pm$  SEM from three independent experiments. pAkt/Akt ratios in each experiment were normalized to that seen in cells expressing wild-type p110 $\beta$  and transfected with GFP-CA-Rac-1, but treated with 0.1% DMSO. (C) Stable p110 $\beta$  knockdown cells were transiently transfected with wild-type p110 $\beta$  without or with GFP-CA-Rac1. After 48 h, cells were treated for 15 min with 0.5  $\mu$ M Latrunculin B, lysed and blotted for p110 $\beta$ , Akt and pT308-Akt. (D) Quantitation of pAkt/Akt immunoblots in Figure 6C. pAkt/Akt ratios in each experiment were normalized to that seen in cells expressing wild-type p110 $\beta$  and GFP-CA-Rac1. The data represent the mean  $\pm$  SD from two independent experiments. (E) Stable p110 $\beta$  knockdown cells were transiently transfected with wild-type p110 $\beta$ , p110 $\beta^{KK-DD}$  or p110 $\beta^{RBD}$ . After 48 h, cells were starved overnight, treated with 25  $\mu$ M EIPA for 3 h, and stimulated for 5 min with 10  $\mu$ M LPA. Cells were lysed and blotted for p110 $\beta$ , Akt and pT308-Akt. (F) Quantitation of pAkt/Akt immunoblots in Figure 6E. pAkt/Akt ratios in each experiment were normalized to that seen in cells expressing wild-type p110 $\beta$  and stimulated with LPA but treated with DMSO. The data represent the mean  $\pm$  SEM from three independent experiments. \* $P$  < 0.05; \*\* $P$  < 0.01; \*\*\* $P$  < 0.001; ns: not significant. Note: The western blot data in Figures 4A and 6A are taken from the same set of experiments, as are the data in Figures 3C and 6E. In each case, cells were treated with 0.1% DMSO or 25  $\mu$ M EIPA. The EIPA arms of these experiments are presented separately in Figure 6, for clarity of the narrative. Because of this, blots for the controls (cells expressing wild-type p110 $\beta$  and treated with DMSO) are shown in Figures 4 and 3, and are not reproduced in Figure 6. We have included the quantitation of

the controls (labeled DMSO) from Figures 3D and 4B in the bar graphs shown in Figure 6B,F, to facilitate a comparison of DMSO- versus EIPA-treated cells.

Author Manuscript

Author Manuscript

Author Manuscript

Author Manuscript